

# Outage Performance of Transdermal Optical Wireless Links in the Presence of Pointing Errors

Stylianos E. Trevlakis\*, Alexandros-Apostolos A. Boulogeorgos\*,<sup>†</sup>, and George K. Karagiannidis\*

\*Department of Electrical and Computer Engineering, Aristotle University of Thessaloniki, Thessaloniki, Greece, 54124

<sup>†</sup>Department of Digital Systems, University of Piraeus, Piraeus, Greece, 18534

Emails: {trevlakis; geokarag}@auth.gr; al.boulogeorgos@ieee.org

**Abstract**—This paper studies the outage performance of transdermal optical wireless communication (OWC) links, in the presence of pointing errors. In this sense, we present a novel tractable path-gain model, which is derived through respective experimental results. Based on this model, we provide the theoretical framework that evaluates and quantifies the impact of pointing errors on transdermal OWC links. In more detail, we obtain a closed-form expression for the outage probability of the optical wireless transdermal link, which takes into account the channel particularities, the transmitter-receiver misalignment, the characteristics of the optical units, as well as, the physical constraints of the in-body device. The results reveal that pointing errors drastically affect the reliability and effectiveness of the link and should be taken into consideration when designing a transdermal OWC link.

**Index Terms**—Outage probability, Optical wireless communications, Performance analysis, Pointing errors, Transdermal optical links

## I. INTRODUCTION

Recent advances in optical wireless communications (OWCs) as well as the lower radio frequency spectrum scarcity and strick regulations [1], [2], motivated by the development of medical implants (MIs) for real-time in-body signal monitoring and human organs' stimulation bandwidth-hungry applications ([3], [4] and references therein). OWCs provide high data rates with low transmission power demands, while, at the same time, they have extremely high immunity to external interference.

As a consequence, great amount of effort has been put to validate and analyze the feasibility and effectiveness of optical wireless transdermal communications [5]–[9]. Specifically, in [5], the authors validated the feasibility of the transdermal optical link (TOL). Additionally, in [6], significant experimental results of direct and retroreflection TOL configurations, were presented, whereas, in [8], the authors evaluated the system model of a transdermal wireless optical link with regard to tissue thickness, data rate and transmitted power. Although, these papers validated the feasibility of the TOL, they neglected the impact of pointing errors, which is expected to play a decisive role in realistic out- to in-body applications. On the other hand, [7] and [9] employed deterministic models to evaluate the effect of pointing errors, in terms of bit error rate. The disadvantage of these models is that, due to their deterministic nature, they are unable to accommodate the stochastic behavior of this phenomenon caused by the relative

motion between the transmitter (TX) and the receiver (RX). Very recently, in [10], the authors considered the stochastic nature of the TOL and derived closed-form expressions for the average signal-to-noise-ratio (SNR), which quantifies the impact of pointing errors.

Motivated by the above, this paper investigates the impact of pointing errors on the system's outage performance. In particular, we present a novel tractable path gain model, which is extracted by employing experimental results. Based on this model, we derive closed-form expressions for the outage probability, which accommodate the transdermal optical channel particularities, the transceivers characteristics, as well as the intensity of pointing errors. These expressions provide important technical insights and the appropriate mathematical tools that can be effectively used for transdermal OWC systems' design.

The rest of this paper is organized as follows. Section II is devoted in presenting the system model and the characteristics of the transdermal optical channel, while, Section III focuses on providing the theoretical framework, which quantifies the TOL's quality in terms of outage probability. Finally, respective numerical results and discussions are provided in Section IV, whereas closing remarks are summarized in Section V.

## II. SYSTEM AND CHANNEL MODEL

As illustrated in Fig. 1, we consider an transdermal transmission setup, in which the external unit emits stimulation messages to the internal unit through the skin. In more detail, it is assumed that the transmitted signal,  $x$ , convey over a wireless channel,  $h$ , with additive noise  $n$ . Hence, the baseband equivalent received signal can be expressed as

$$y = \eta hx + n, \quad (1)$$

where  $\eta$  is the photodiode's efficiency and  $n$  is modelled as a zero-mean complex Gaussian process with variance  $\sigma^2$ .

The channel,  $h$ , can be expressed as in [6]

$$h = h_l h_p, \quad (2)$$

where  $h_l$  and  $h_p$  respectively stand for the deterministic channel coefficient, due to the propagation loss, and the stochastic process that models the geometric spread, because of the so-called *misalignment fading*. We assume a Gaussian spatial intensity profile of  $w_\delta$  on the RX plane at distance  $\delta$  from the TX and circular aperture of radius  $\beta$ . Furthermore,

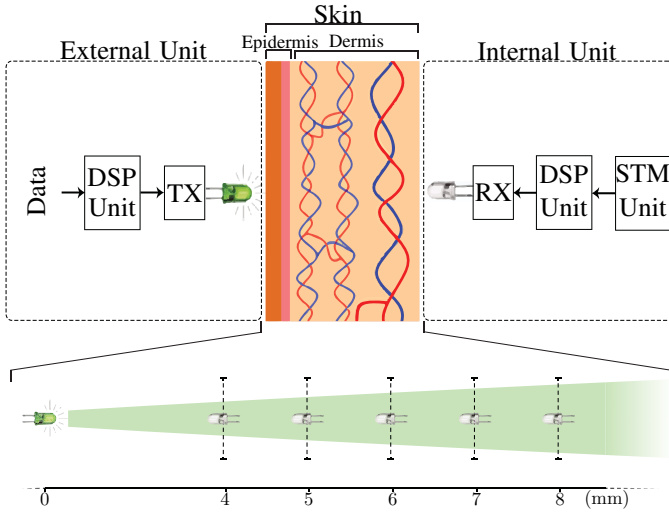


Fig. 1: System model.

 TABLE I: The  $a_i$ ,  $b_i$  and  $c_i$  values.

$i$	$a_i$	$b_i$	$c_i$
1	10	0.35	0.065
2	4.5	0.42	0.25
3	13.48	-1.5	50.12
4	14.7	1442	49.35
5	7.435	1499	75.88
6	48	3322	1033
7	594.1	-183	285.9
8	11.47	-618.5	1054

the stochastic term of the channel coefficient,  $h_p$ , represents the fraction of the collected power due to geometric spread with radial displacement  $r$  from the origin of the detector. Moreover, by assuming that the elevation and the horizontal displacement (sway) follow independent and identical Gaussian distributions, as in [11], we observe that the radial displacement at the RX follows a Rayleigh distribution. As a result, the probability density function (PDF) of the random variable  $h_p$  can be obtained as in [12],

$$f_{h_p}(x) = \frac{\xi}{A_0^\xi} x^{\xi-1}, \quad 0 \leq x \leq A_0, \quad (3)$$

where,

$$A_0 = \text{erf}(v)^2, \quad (4)$$

stands for the the fraction of the collected power in case of zero radial displacement [13], with

$$v = \frac{\sqrt{A}}{\sqrt{2}w_\delta}, \quad (5)$$

where,  $A$  and  $w_\delta$  respectively denote the RX's photodiode effective area and the beam waste (radius calculated at  $e^{-2}$ )

on the RX plane at distance  $\delta$  from the TX. Likewise,  $\xi$  is the square ratio of the equivalent beam radius,  $w_{eq}$ , and the pointing error displacement standard deviation at the RX, which can be expressed as

$$\xi = \frac{w_{eq}^2}{4\sigma_s^2}, \quad (6)$$

where  $\sigma_s^2$  is the pointing error displacement (jitter) variance at the RX. Finally,  $w_{eq}^2$  can be evaluated as

$$w_{eq}^2 = w_\delta^2 \frac{\sqrt{\pi} \text{erf}(v)}{2v \exp(-v^2)}. \quad (7)$$

Finally, the cumulative distribution function (CDF) of  $h_p$  can be obtained as

$$F_{h_p}(x) \triangleq \int_0^x f_{h_p}(y) dy = \begin{cases} \frac{1}{A_0^\xi} x^\xi & 0 \leq x \leq A_0 \\ 1, & x \geq A_0 \end{cases}. \quad (8)$$

By using the basics of statistics, the CDF of  $h_p^2$  can be obtained as

$$F_{h_p^2}(x) = F_{h_p}(\sqrt{x}), \quad (9)$$

which, by employing (8), can be rewritten as

$$F_{h_p^2}(x) = \begin{cases} \frac{1}{A_0^\xi} x^{\xi/2} & 0 \leq x \leq A_0^2 \\ 1, & x \geq A_0^2 \end{cases}, \quad (10)$$

while, the PDF of  $h_p^2$  can be obtained as

$$f_{h_p^2}(x) = \frac{dF_{h_p^2}(x)}{dx} = \frac{\xi}{2A_0^\xi} x^{\xi/2-1}. \quad (11)$$

On the other hand, the deterministic term of the channel coefficient can be expressed as [4, eq. (10.1)]

$$h_t = \exp\left(-\frac{1}{2}\alpha(\lambda)\delta\right), \quad (12)$$

where  $\alpha(\lambda)$  and  $\delta$  represent the skin attenuation coefficient in the wavelength  $\lambda$ , and the total dermis thickness, respectively. Note that the values of  $\alpha(\lambda)$  depend on the optical properties of the skin and can be obtained from [14] and [15]. Based on these values and, by employing the trust region method, we obtain the following novel closed-form expression for the skin attenuation coefficient in the region of [400, 1800 nm],

$$\alpha(\lambda) = \sum_{i=1}^8 a_i \exp\left(-\left(\frac{\lambda - b_i}{c_i}\right)^2\right), \quad (13)$$

where the values of  $a_i$ ,  $b_i$  and  $c_i$ , with  $i = 1, \dots, 8$ , are provided in Table I, whereas  $\lambda$  is given in nm. Note that, the accuracy of this expression is more than 99.7%.

### III. OUTAGE PROBABILITY

In order to evaluate the reliability of the TOL, we study its outage performance. In this sense, the following theorem returns the outage probability of the link as a function of the average SNR and the link's intensity.

*Theorem 1:* The outage probability can be expressed as

$$P_o(\gamma_{th}) = \begin{cases} \left(\frac{\xi}{\xi+2}\right)^{\xi/2} \tilde{\gamma}^{-\xi/2} \gamma_{th}^{\xi/2}, & \text{if } \gamma_{th} \leq \frac{\xi+2}{\xi} \tilde{\gamma}, \\ 1, & \text{otherwise} \end{cases} \quad (14)$$

where  $\gamma_{th}$  and  $\tilde{\gamma}$  respectively stand for the SNR threshold and the average SNR, which can be obtained as

$$\tilde{\gamma} = \frac{\xi A_0^2 \eta^2 \exp(-\alpha(\lambda)\delta) \tilde{P}_s}{(\xi+2) N_0}. \quad (15)$$

*Proof:* Please refer to the Appendix. ■

From (14), it is evident that, for a given  $\gamma_{th}$  and  $\tilde{\gamma}$ , as  $A_0$  increases, the outage performance of the system improves. Moreover, it is evident that, for a fixed  $\gamma_{th}$  and  $A_0$ , as  $\tilde{\gamma}$  increases, the outage probability decreases. Finally, it is observed that as  $\gamma_{th}$  increases, i.e., as the modulation order increases, the outage probability also increases. If  $\gamma_{th}$  exceeds a certain limit, the system is always in an outage condition. This indicates the importance of taking into account the impact of pointing errors when selecting the modulation order.

### IV. RESULTS AND DISCUSSION

In this section, we evaluate the performance of the TOL by illustrating analytical and Monte-Carlo simulation results for different insightful scenarios. In more detail, we assume that the photodiode effective area,  $A$ , is  $1 \text{ mm}^2$ , while the divergence angle,  $\theta$ , equals  $20^\circ$ . Additionally, unless otherwise is stated, the skin thickness,  $\delta$ , is set equal to  $4 \text{ mm}$ , while the noise optical PSD,  $N_0$ , is  $(1.3 \text{ pA}/\sqrt{\text{Hz}})^2$  [16]. The beam waist in distance  $\delta$  is calculated as

$$w_\delta = \delta \tan\left(\frac{\theta}{2}\right). \quad (16)$$

Finally, we assume that  $\tilde{P}_s = 0.1 \text{ } \mu\text{W}/\text{MHz}$ ,  $\lambda = 1100 \text{ nm}$  and  $\xi = 1$ .

In Fig. 2, the outage probability is illustrated as a function of the normalized SNR for different values of  $\xi$ . Note that the normalized SNR is defined as

$$\hat{\gamma} = \frac{2\pi}{e} \frac{\tilde{\gamma}}{\gamma_{th}}. \quad (17)$$

In this figure, markers are used to illustrate the simulation outcomes, whereas the corresponding continuous lines are employed for analytical results. It is evident that the analytical results are identical with the corresponding simulations; thus, verifying the presented analytical framework. Additionally, we observe that, for a fixed normalized SNR, the outage probability increases as the effect of pointing errors become more severe, i.e., as the level of alignment,  $\xi$ , decreases. Moreover, as expected, for a given  $\xi$ , the outage performance

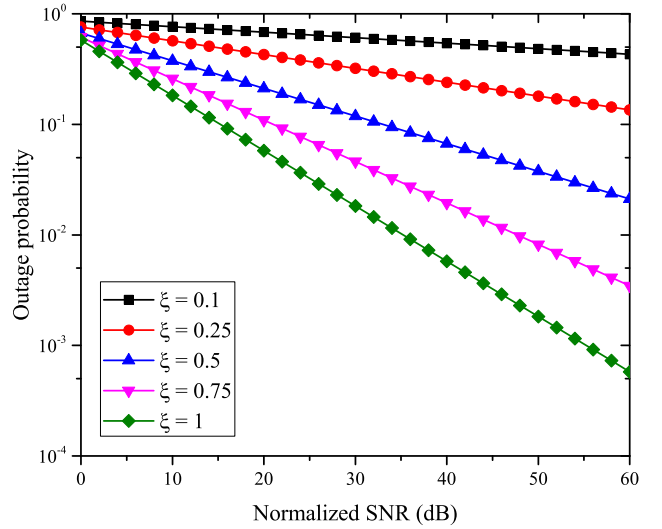


Fig. 2: Outage probability vs normalized SNR for different values of  $\xi$ .

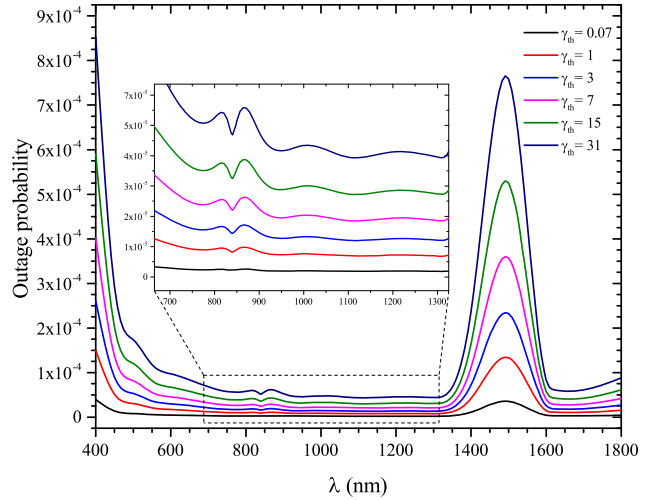


Fig. 3: Outage probability vs wavelength for different values of SNR threshold.

improves, as the normalized SNR increases. Finally, as the normalized SNR increases, the pointing errors have a more detrimental effect on the outage probability. For example, for a normalized SNR equal to 10 and 50 dB, the outage probability degrades about 76% and 99%, respectively, when  $\xi$  is altered from 0.1 to 1. This indicates the importance of taking into consideration the impact of pointing errors, when selecting the transmission power and spectral efficiency.

Fig. 3 depicts the outage probability as a function of the wavelength for different values of SNR threshold, assuming that the transmission signal PSD equals  $0.1 \text{ } \mu\text{W}/\text{MHz}$  and  $\xi = 1$ . As expected, for a fixed wavelength, as  $\gamma_{th}$  increases, the outage probability also increases. For example, for  $\lambda = 600 \text{ nm}$ , the outage probability increases approximately 20%, as  $\gamma_{th}$  is altered from 0.07 to 31. Additionally, from

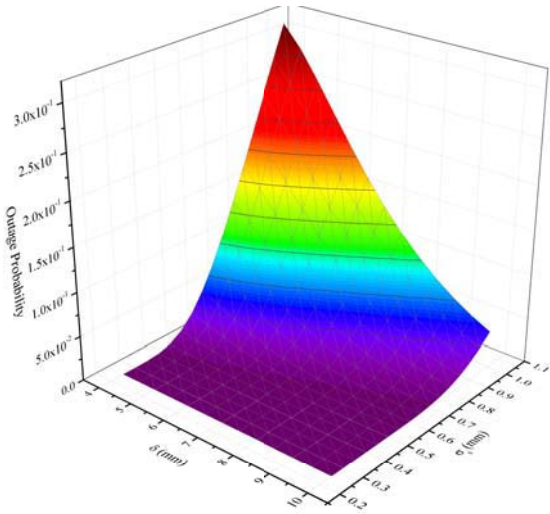


Fig. 4: Outage probability vs skin thickness and jitter standard deviation, for  $\gamma_{th} = 3$ .

In this figure, it is evident that a transmission window exists for wavelengths between 700 and 1300 nm. Note that, in this wavelength region several commercial light emitting diodes and photodetectors exist (see for example [17], [18]). Finally, we observe that the wavelength windows from 400 to 600 nm and around 1500 nm are not optimal for OWCs, whereas the optimal transmission wavelength is 1100 nm.

In Fig. 4, the outage probability is depicted as a function of the skin thickness and the jitter standard deviation, assuming that  $\gamma_{th} = 3$ . From this figure, it is evident that in the low  $\delta$  regime, the impact of pointing errors is more detrimental than in the high  $\delta$  regime. This is expected, since, as illustrated in Fig. 1, for a fixed spatial jitter, as  $\delta$  increases, the probability that the RX is within the transmission effective area also increases. However, as  $\delta$  increases, the path gain also increases. In other words, we observe that the impact of pointing errors is more significant than the effect of path gain, for realistic values of  $\delta$ .

Fig. 5 illustrates the outage probability as a function of skin thickness for different values of SNR threshold,  $\gamma_{th}$ , for  $\lambda = 1500$  nm. We observe that the analytical and simulation results coincide; therefore, the analytical framework for the derivation of the outage probability is verified. We observe that for a fixed skin thickness, as  $\gamma_{th}$  increases, the outage probability also increases. For example, for  $\delta = 8$  mm and  $\gamma_{th} = 0.5$ , the outage probability is in the order of  $10^{-9}$ , while for the same  $\delta$  and  $\gamma_{th} = 3$ , the outage probability is in the order of  $10^{-2}$ . Furthermore, for the same  $\gamma_{th}$ , when  $\delta$  alters from 4 to 8 mm, the outage probability decreases. On the contrary, for the same  $\gamma_{th}$ , when  $\delta$  exceeds 8 mm, the outage probability increases. This is because, the pointing errors drastically affect the transmission at closer TX-RX distance. In other words, as the skin thickness increases, the effect of the pointing errors decreases, whereas the impact of path gain becomes more severe.

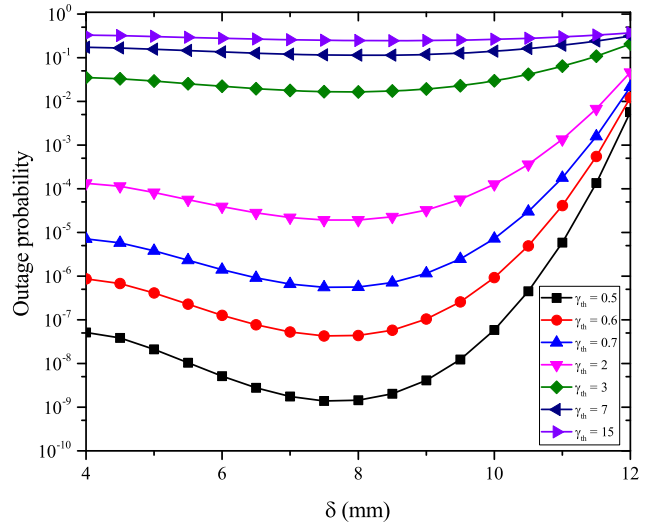


Fig. 5: Outage probability vs skin thickness for different values of SNR threshold, for  $\lambda = 1500$  nm.

## V. CONCLUSIONS

In this paper, we first presented a novel tractable path gain model, which is extracted through experimental results. Based on this model, we provided novel closed-form expressions for the outage probability in transdermal OWCs, which take into account the channel particularities, the characteristics of the optical transceivers, as well as, their misalignment. Our results reveal the existence of an ultrawideband transmission window in the range of 700 to 1300 nm. In addition, the optimal transmission wavelength is 1100 nm. Finally, the effect of pointing errors is proven to be detrimental and can degrade the transdermal OWC performance more than 10%.

## APPENDIX

Based on (1), (12), and by assuming an intensity modulation and direct detection (IM/DD) method, the instantaneous SNR can be obtained as [19]

$$\gamma = \frac{\eta^2 \exp(-\alpha(\lambda)\delta) h_p^2 P_s}{\sigma^2}, \quad (18)$$

$$= \frac{\eta^2 \exp(-\alpha(\lambda)\delta) h_p^2 \tilde{P}_s}{N_0}, \quad (19)$$

where  $P_s$  denotes the average optical power of the transmitted signal, whereas  $\tilde{P}_s$  and  $N_0$  respectively represent the signal and noise optical power spectral density (PSD).

According to (19), the instantaneous SNR is a random variable (RV) that follows the same distribution as  $h_p^2$ . Therefore, in order to derive the average SNR of the optical link, we first need to identify the distribution of  $h_p^2$ .

Furthermore, we recall that the outage probability is defined as the probability of the SNR,  $\gamma$ , to fall below a corresponding predetermined threshold,  $\gamma_{th}$ , i.e.,

$$P_o(\gamma_{th}) = P_r(\gamma \leq \gamma_{th}). \quad (20)$$

With the aid of (19), (20) can be rewritten as

$$P_o(\gamma_{th}) = P_r \left( h_p^2 \leq \frac{N_0 \gamma_{th}}{\eta \exp(-\alpha(\lambda)\delta) \bar{P}_s} \right), \quad (21)$$

or

$$P_o(\gamma_{th}) = F_{h_p^2} \left( \frac{N_0 \gamma_{th}}{\eta \exp(-\alpha(\lambda)\delta) \bar{P}_s} \right), \quad (22)$$

which by employing (10) can be rewritten as (14).

#### REFERENCES

- [1] A.-A. A. Boulogeorgos, "Interference mitigation techniques in modern wireless communication systems," Ph.D. dissertation, Aristotle University of Thessaloniki, Thessaloniki, Greece, Sep. 2016.
- [2] A.-A. A. Boulogeorgos and G. K. Karagiannidis, "Low-cost cognitive radios against spectrum scarcity," *IEEE Technical Committee on Cognitive Networks Newsletter*, vol. 3, no. 2, pp. 30–34, Nov. 2017.
- [3] Z. Ghassemlooy, S. Arnon, M. Uysal, Z. Xu, and J. Cheng, "Emerging optical wireless communications—advances and challenges," *IEEE J. Sel. Areas Commun.*, vol. 33, no. 9, pp. 1738–1749, Sep. 2015.
- [4] M. Faria, L. N. Alves, and P. S. de Brito André, *Transdermal Optical Communications*. CRC Press, Jun. 2017, vol. 1, ch. 10, pp. 309–336.
- [5] J. L. Abita and W. Schneider, "Transdermal optical communications," *JOHNS HOPKINS APL TECHNICAL DIGEST*, vol. 25, no. 3, p. 261, 2004.
- [6] Y. Gil, N. Rotter, and S. Arnon, "Feasibility of retroreflective transdermal optical wireless communication," *Appl Opt*, vol. 51, no. 18, pp. 4232–4239, Jun. 2012.
- [7] T. Liu, U. Bihl, S. M. Anis, and M. Ortmanns, "Optical transcutaneous link for low power, high data rate telemetry," in *Annual International Conference of the IEEE Engineering in Medicine and Biology Society (EMBC)*. IEEE, Aug. 2012, pp. 3535–3538.
- [8] T. Liu, J. Anders, and M. Ortmanns, "System level model for transcutaneous optical telemetric link," in *IEEE International Symposium on Circuits and Systems (ISCAS)*, May 2013, pp. 865–868.
- [9] T. Liu, U. Bihl, J. Becker, J. Anders, and M. Ortmanns, "In vivo verification of a 100 mbps transcutaneous optical telemetric link," in *IEEE Biomedical Circuits and Systems Conference (BioCAS)*, Oct. 2014, pp. 580–583.
- [10] S. E. Trevlakis, A.-A. A. Boulogeorgos, and G. K. Karagiannidis, "On the impact of misalignment fading in transdermal optical wireless communications," in *7th International Conference on Modern Circuits and Systems Technologies*, May 2018.
- [11] S. Arnon, "Effects of atmospheric turbulence and building sway on optical wireless-communication systems," *Opt. Lett.*, vol. 28, no. 2, pp. 129–131, Jan. 2003.
- [12] H. G. Sandalidis, T. A. Tsiftsis, G. K. Karagiannidis, and M. Uysal, "Ber performance of FSO links over strong atmospheric turbulence channels with pointing errors," *IEEE Commun. Lett.*, vol. 12, no. 1, pp. 44–46, Jan. 2008.
- [13] A. A. Farid and S. Hranilovic, "Outage capacity optimization for free-space optical links with pointing errors," *J. Lightwave Technol.*, vol. 25, no. 7, pp. 1702–1710, Jul. 2007.
- [14] A. N. Bashkatov, E. A. Genina, and V. V. Tuchin, "Optical properties of skin, subcutaneous, and muscle tissues: a review," *Journal of Innovative Optical Health Sciences*, vol. 4, no. 01, pp. 9–38, Jan. 2011.
- [15] A. Bashkatov, E. Genina, V. Kochubey, and V. Tuchin, "Optical properties of human skin, subcutaneous and mucous tissues in the wavelength range from 400 to 2000 nm," *J. Phys. D: Appl. Phys.*, vol. 38, no. 15, p. 2543, Jul. 2005.
- [16] *155Mbps Low-Noise Transimpedance Amplifier*, Maxim Integrated Products, Feb. 2004, rev. 2.
- [17] *High Speed Infrared Emitting Diode, 830 nm, GaAlAs Double Hetero*, Vishay Semiconductors, Aug. 2011, rev. 1.2.
- [18] *Infrared (IR) Emitter 940nm 1.2V 100mA 7.8mW/sr @ 20mA 20° Radial*, Everlight Electronics Co Ltd, Dec. 2016, rev. 5.
- [19] S. Arnon, J. Barry, G. Karagiannidis, R. Schober, and M. Uysal, Eds., *Advanced Optical Wireless Communication Systems*, 1st ed. New York, NY, USA: Cambridge University Press, May 2012.